OPEN ACCESS
CellPress

Cell Reports
Report

The APC Network Regulates the Removal of Mutated Cells from Colonic Crypts

Je-Hoon Song,[1] David J. Huels,[2] Rachel A. Ridgway,[2] Owen J. Sansom,[2] Boris N. Kholodenko,[3,4,5] Walter Kolch,[3,4,5] and Kwang-Hyun Cho[1,*]

[1]Department of Bio and Brain Engineering, Korea Advanced Institute of Science and Technology (KAIST), 291 Daehak-ro, Yuseong-gu, Daejeon 305-701, Republic of Korea
[2]The Beatson Institute for Cancer Research, Garscube Estate, Glasgow G61 1BD, UK
[3]Systems Biology Ireland, University College Dublin, Belfield, Dublin 4, Ireland
[4]Conway Institute of Biomolecular and Biomedical Research, University College Dublin, Belfield, Dublin 4, Ireland
[5]School of Medicine and Medical Science, University College Dublin, Belfield, Dublin 4, Ireland
*Correspondence: ckh@kaist.ac.kr
http://dx.doi.org/10.1016/j.celrep.2014.02.043

SUMMARY

Self-renewal is essential for multicellular organisms but carries the risk of somatic mutations that can lead to cancer, which is particularly critical for rapidly renewing tissues in a highly mutagenic environment such as the intestinal epithelium. Using computational modeling and in vivo experimentation, we have analyzed how adenomatous polyposis coli (APC) mutations and β-catenin aberrations affect the maintenance of mutant cells in colonic crypts. The increasing abundance of APC along the crypt axis forms a gradient of cellular adhesion that causes more proliferative cells to accelerate their movement toward the top of the crypt, where they are shed into the lumen. Thus, the normal crypt can efficiently eliminate β-catenin mutant cells, whereas APC mutations favor retention. Together, the molecular design of the APC/β-catenin signaling network integrates cell proliferation and migration dynamics to translate intracellular signal processing and protein gradients along the crypt into intercellular interactions and whole-crypt physiological or pathological behavior.

INTRODUCTION

Although self-renewal is essential for multicellular organisms, it bears the risk of mutations, in particular, in environments with high concentrations of mutagens such as the colon (Azcárate-Peril et al., 2011; Diggs et al., 2011; Pearson et al., 2009). The human colorectal epithelium is renewed every 2–3 days (Okamoto and Watanabe, 2004) making it a vulnerable target for carcinogenesis, and colorectal cancer (CRC) is the third most frequent cancer worldwide (Ferlay et al., 2010). The regeneration of the colorectal epithelium is maintained by a proliferating unit termed crypt (Humphries and Wright, 2008). The adult colon contains 10^7 crypts, and each crypt consists of 1,000–4,000 cells. In order to regenerate such a huge cell population over many decades without malignant aberrations, crypts may have evolved mechanisms to minimize the cancer risk. Such strategies may include the spatiotemporal organization of cell proliferation, migration, and differentiation (Gatenby et al., 2010; Nowak et al., 2003). Cancer prevention being a built-in design feature of epithelial anatomy is an attractive hypothesis, but the molecular mechanisms remain to be elucidated.

Crypt cell proliferation is controlled by a spatial gradient of extracellular Wnt ligands, which causes the differential distribution of proliferative cells along the crypt axis (Davies et al., 2008; Murray et al., 2010; van de Wetering et al., 2002). In the absence of Wnt, cytoplasmic β-catenin is constantly degraded by the destruction complex (DC), which is composed of Axin, adenomatous polyposis coli (APC), and GSK3β. Binding of Wnt to its receptor Frizzled inhibits the DC, leading to the stabilization of β-catenin, which translocates to the nucleus and in conjunction with T cell factor/lymphoid enhancer factor (TCF/LEF) regulates the transcription of >100 genes that control cell proliferation. On the other hand, β-catenin can bind to E-cadherin forming an adhesion complex that controls cell-cell adhesion and migration. Such dual functions of β-catenin imply an integrated regulation of proliferation and migration for maintaining the homeostasis of crypt cells, which so far were analyzed in separation.

APC mutation in the Wnt pathway is the earliest genetic alteration in CRC (Powell et al., 1992), but it takes years to decades for a cancer to develop (Fearon, 2011). Germline APC mutations cause familial adenomatous polyposis (FAP), which eventually results in CRC in the third to fifth decade of life. This long latency suggests a robust tumor defense that may include the requirement for additional mutations, a residual tumor suppressive function of mutated APC, and the effective elimination of mutated cells (Fearon, 2011; Muzny et al., 2012; Segditsas and Tomlinson, 2006). Although the analysis of accumulating mutations has dominated the field, tumor suppressive mechanisms are equally important. For instance, Wnt activation during CRC pathogenesis occurs in two steps, the first being APC mutation, whereas the second seems to optimize the transcriptional output of Wnt signaling for tumor progression (Najdi et al., 2011). APC mutations promote β-catenin translocation to the nucleus (Sansom et al., 2004), although the quantitative extent is modulated

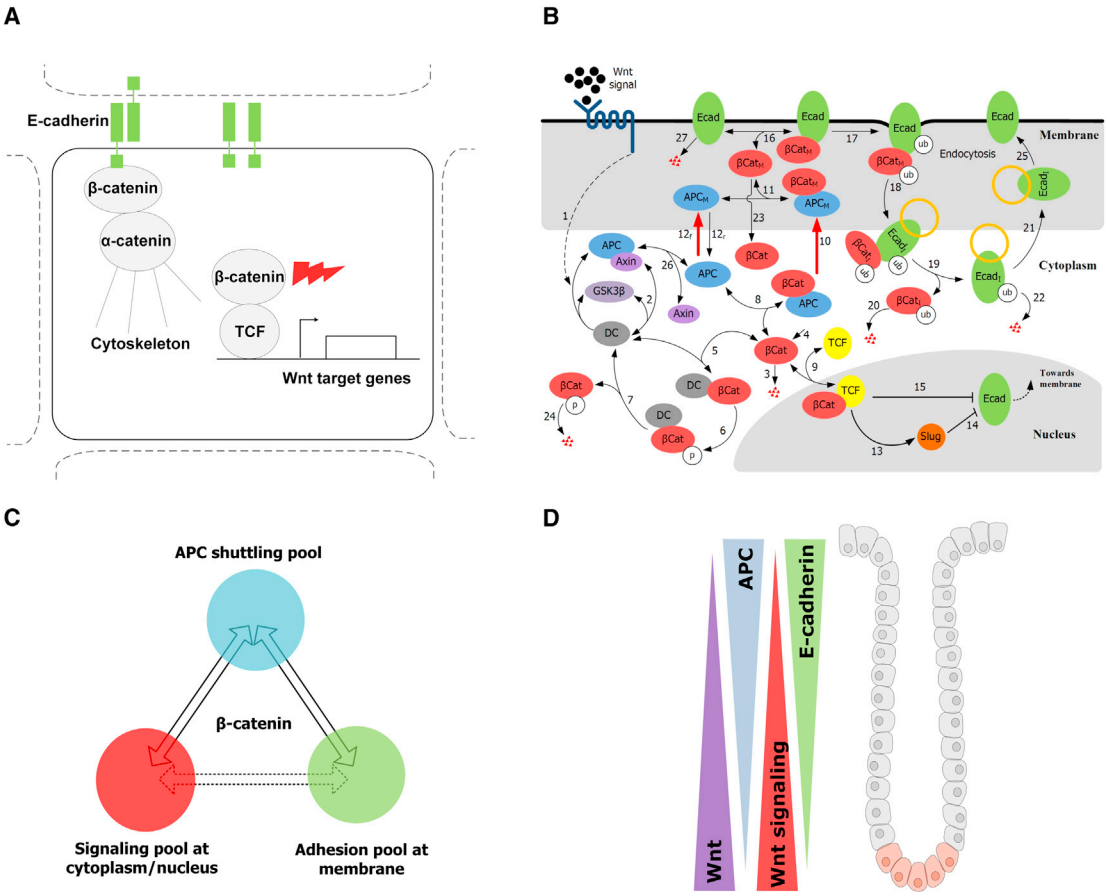

Figure 1. Scheme of the Mathematical β-Catenin Model and Factors Considered in the Construction of the Model

(A) Schematic diagram showing that β-catenin is a key component of both the Wnt signaling pathway and the E-cadherin cell adhesion complex.

(B) A reaction scheme of our mathematical model, which consists of β-catenin destruction, β-catenin/TCF nuclear signaling, APC shuttling, and adhesion complex remodeling.

(C) β-catenin exchanges between three distinct molecular pools within a cell.

(D) Molecular gradients within the colonic crypt. Stem cells (red) at the bottom of the crypt replenish colonic epithelial cells (gray) that differentiate as they move upward.

by other, poorly understood factors. APC mutated tumors retain membrane β-catenin comparable to normal epithelium in the tumor center, whereas cells at the invasive front show nuclear β-catenin (Brabletz et al., 1998; Phelps et al., 2009). This observation suggests that the effects of mutations are modulated by a dynamic competition between tumor promoting and suppressive forces that may depend on the signaling status of individual cells and their local microenvironment.

To analyze this hypothesis, we integrated all available experimental evidence and developed a mathematical model that allowed us to simulate the coordination between the adhesion and signaling function of β-catenin, and the adhesion and migration of single cells in normal, β-catenin, and APC mutated colonic crypts. Our results reveal a tumor suppressing function arising from the interactions between dynamic subcellular APC network and the adhesion gradient in the crypt, which promotes the elimination of mutant cells with high Wnt signaling. Subversion of these interactions permits mutant cells to persist in the crypt and initiate CRC.

RESULTS

Construction of a Mathematical Model for the Dynamic Analysis of Multiple β-Catenin Functions

We developed a mathematical model (Figure 1) that allowed us to investigate the dynamics of (1) the Wnt signaling pathway and resulting suppression of E-cadherin transcription; (2) the formation of functional E-cadherin-β-catenin adhesion complexes at the cell membrane; (3) the removal and recycling of E-cadherin-β-catenin adhesion complexes by endocytosis; and (4) the role of APC in coordinating the participation of β-catenin in adhesion versus Wnt signaling (see Supplemental Results for details).

We report the following key features of Wnt-E-cadherin system. First, the premise that β-catenin can be removed by degradation from the adhesion pool, but not from the signaling pool establishes a continuous flux of β-catenin from the signaling to the adhesion pool, which counterbalances the Wnt-induced formation of the β-catenin:TCF complex (Figure 2). This explains the

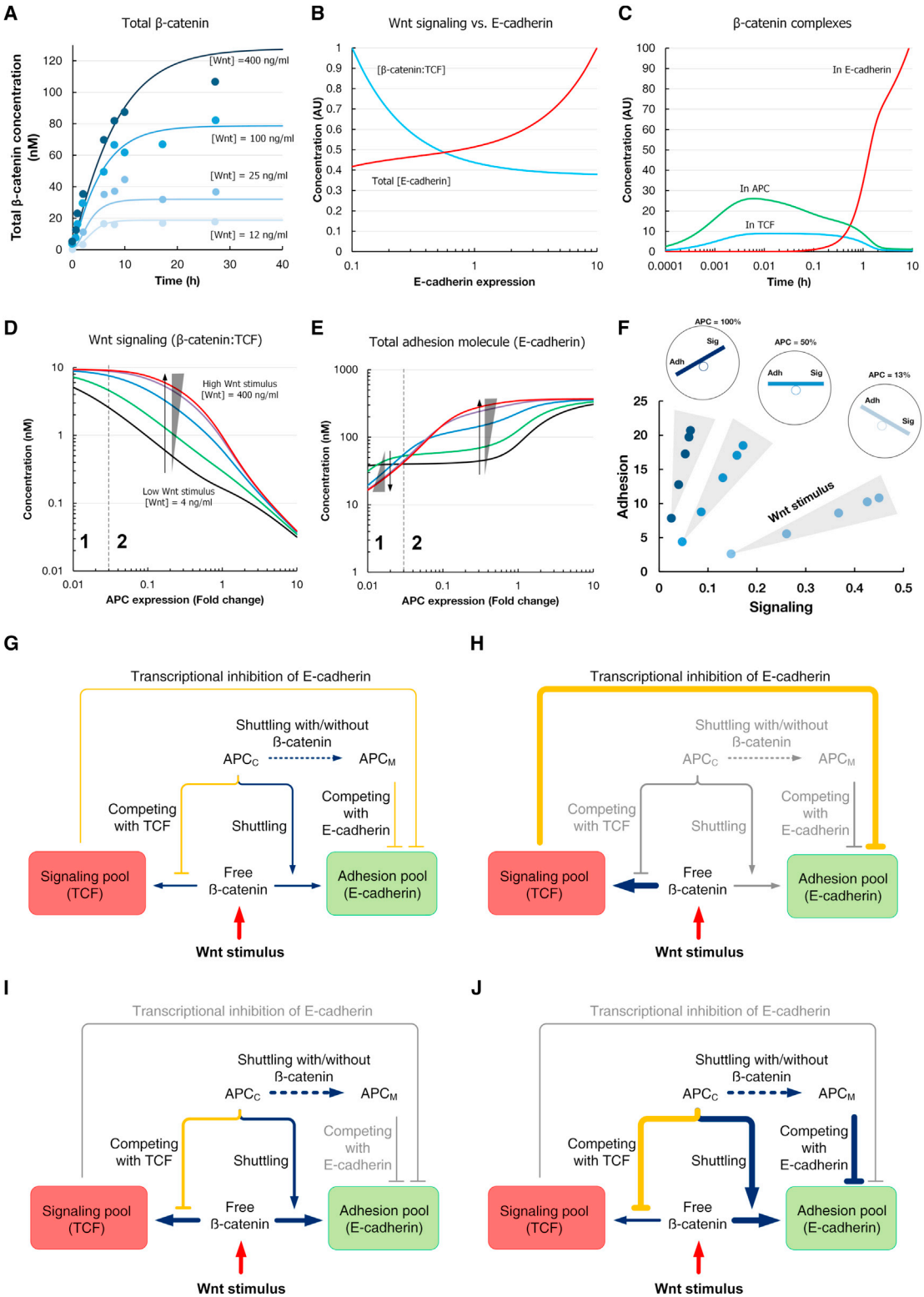

Figure 2. APC Regulates the Distribution of β-Catenin between Signaling and Adhesion Pools

(A) Profiles of β-catenin abundance in response to Wnt stimulation in E-cadherin-negative cells.

(B) Increasing E-cadherin expression (A_E) represses Wnt signaling by decreasing the abundance of the β-catenin:TCF complex.

(legend continued on next page)

experimental observation that E-cadherin can downregulate the signaling function of β-catenin even when a Wnt stimulus is present (Herzig et al., 2007). Second, the stimulatory effect of Wnt signaling on adhesion complex formation arises from the effect that the basal level degradation rate of E-cadherin is higher than that of ubiquitinated E-cadherin (or of complexed E-cadherin), so that its binding to β-catenin protects E-cadherin from degradation (Figure 2E). Third, the ratio of β-catenin within signaling complex to that within adhesion complex is controlled by APC expression levels (Figure 2F) (see Supplemental Results for details).

We further extended our analysis of cellular dynamics to the level of simulating cell migration within a crypt by constructing a mathematical model of "individually migrating cell" (IMC) (Figures 3A–3C). We confirmed that the IMC model could reproduce the changes in Wnt signaling (as measured by the formation of the β-catenin:TCF complex), E-cadherin, and β-catenin expression profiles along the crypt that are consistent with experimental observations (Figures 3D–3F, 3H, and 3I). We found that the increasing profile of APC plays an essential role in establishing the molecular profiles (β-catenin, E-cadherin, and Wnt activity), and that the adhesion (as measured by the formation of the β-catenin:E-cadherin complex) increased along the crypt axis, whereas the Wnt signaling decreased (first row of Figure 4B and Figures 3G and 3J) (see Supplemental Results for details).

Spatial Signaling and Adhesion Gradients in the Crypt Facilitate the Elimination of Mutated Cells with a High Proliferative Potential

In particular, we investigated the effect of somatic mutations that enhance Wnt signaling and result in cells with a higher proliferative potential than normal neighboring cells (see Figures S4A and S4B for mutation models). Such mutations can also change the amount of adhesion complexes within a cell and subsequently induce a different adhesion level between the mutated cell and its normal neighboring cells. To investigate the effect of this "adhesion difference," we employed a force model based on the differential adhesion (see Supplemental Experimental Procedures), which posits that cells rearrange their positions to minimize the total sum of their adhesion differences (Figure 3C).

We investigated the effect of somatic mutations on a normal crypt (Figure S4B). The de novo synthesis rate of β-catenin (k_4) was perturbed to mimic mutations that enhance Wnt signaling. The model predicted that both signaling and adhesion increase in the mutated cell at every different height of crypt in accord with cell-level results (Figure 2F; first row of Figure 4D). The mutated cell experiences an additional force to move upward because increased adhesion causes an adhesion difference between the mutated cell and its normal neighbors (first rows of Figures 4E and 4F). As a result, mutated somatic cells with enhanced proliferation are expelled from the crypt more quickly than normal cells.

Next, we investigated the effects of APC mutations on stem cells. According to the studies about hereditary colorectal cancer syndromes, APC mutations predispose to CRC, but further alterations are required to cause full malignant transformation, and a key event in this process seems to be the acquisition of the "just right" level of Wnt signaling (Gaspar and Fodde, 2004; Minde et al., 2011; Segditsas and Tomlinson, 2006). Therefore, we simulated the effects of APC mutations in crypt stem cells on the adhesion gradient. As most APC mutations are truncations that can reduce function to different degrees (Cho et al., 2006; Fodde et al., 2001; Gaspar and Fodde, 2004), we considered three cases where the maximum APC expression and function (APC_{Max}) is reduced to 50%, 12%, and 3%, respectively, of its wild-type value (second to fourth rows of Figure 4). The expression profiles of β-catenin and E-cadherin progressively reversed from increasing toward the top of the crypt in wild-type APC crypts to a decrease as APC function was reduced (Figure 4A). These changes correlated with a decrease in the β-catenin adhesion pool, whereas the β-catenin signaling pool was increased (Figure 4B). Thus, a decline in APC function selectively disturbs the adhesion profile of the crypt abolishing the normal adhesion gradient when APC function is reduced by 50%, and even reversing it when APC function is 12% or less. Importantly, if a cell in the mutated crypt had experienced an additional Wnt pathway stimulation the adhesion difference, $A_1(x) - A_0(x)$ still remained positive (second to fourth rows in Figure 4D). So, the enhancement of adhesion by additional β-catenin (due to APC shuttling and the increase of the total number of adhesion molecules [Figure 2E]) is maintained even for the variation of APC function. This means that the cell still would move with the adhesion gradient and reverse direction with the gradient because the reversed adhesion gradient also reverses the direction of the force (second to fourth rows in Figures 4E and 4F). In the case of a crypt where loss of APC function had reversed the adhesion gradient, such an additional Wnt stimulation would counteract the elimination of the affected cell. Based on these results, we suggest that spatial signaling and adhesion

(C) Profile of the temporal relaxation dynamics of β-catenin distribution into its different functional protein complexes under unperturbed conditions (i.e., no Wnt signal and no APC mutations).

(D and E) Steady states of the concentrations of (D) the β-catenin:TCF complex, and (E) total E-cadherin are plotted in dependence of APC expression and Wnt stimulation. Zones 1 and 2 indicate regions that represent distinct response modes to Wnt stimulation. Black line, low Wnt stimulus; green/blue/magenta lines, increasing Wnt stimulus; red line, high Wnt stimulus; arrows in (E), increasing directions of Wnt stimulations in zones 1 and 2, respectively.

(F) Pairs of signaling and adhesion functionalities in response to Wnt stimulus are traced on the phase plane.

(G–J) The dynamic regulation of the balance between the signaling and adhesion pools. (G) The competition between E-cadherin and TCF for binding with β-catenin results in a mutually inhibitory effect between signaling and adhesion functions. The competition is balanced by the efficiency of APC shuttling. In cells with wild-type APC, β-catenin is efficiently transported to the membrane by APC where β-catenin is sequestered in a complex with E-cadherin. If the concentration of functional APC is decreased, e.g., due to mutation, TCF binding to β-catenin increases the transcription of Slug, which suppresses E-cadherin gene expression. (H) For a low level of APC expression, the increased signaling complex by extracellular Wnt stimulus transcriptionally inhibits E-cadherin. (I) For a middle level of APC expression, Wnt stimulus increases both signaling complex and adhesion complex. (J) For a high level of APC expression, APC decreases both signaling and adhesion sensitivities to Wnt stimulus.

See also Figures S1 and S2.

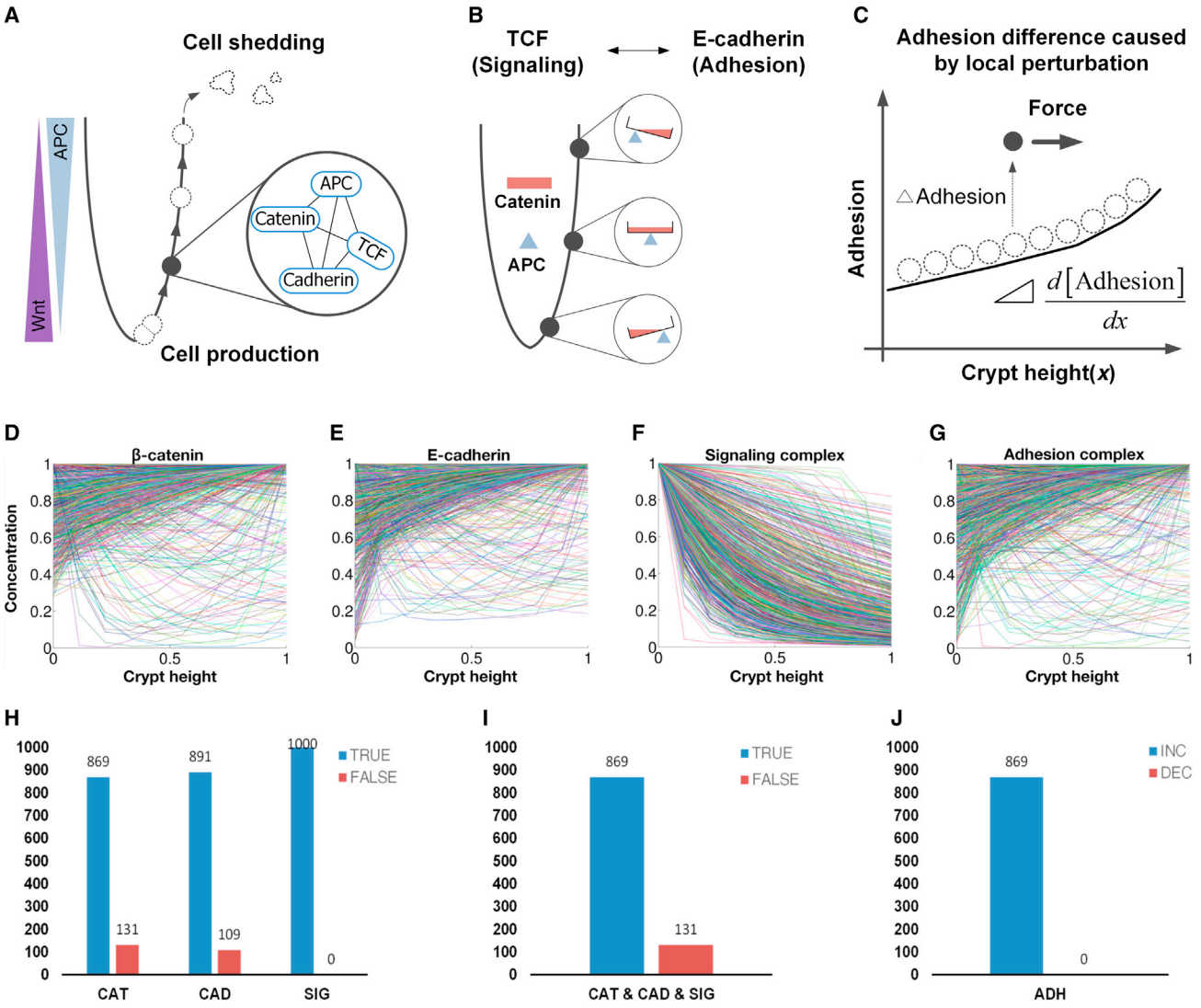

Figure 3. Model of an Individually Migrating Cell Moving up the Crypt

(A) The individually migrating cell (IMC) model assumes that a normal cell is autonomously migrating up the crypt. Therefore, their regulation of the intracellular β-catenin interaction network changes depending on the position of the IMC in the crypt.

(B) Schematic illustration of the balancing role of APC in a crypt. APC negatively regulates the β-catenin:TCF complex, but positively regulates the β-catenin:E-cadherin complex. Thus, the differential APC expression along the crypt controls the functional balance between signaling and adhesion.

(C) A force model governing the position of a cell in an epithelial sheet of tissue.

(D–J) The IMC model simulation using random coefficients for APC and Wnt ligand profile. (D–G) The profiles of β-catenin (D), E-cadherin (E), signaling complex (F), and adhesion complex (G) were produced from the IMC model. (H and I) A large portion of the random coefficients successfully reproduced the qualitative pattern of the profiles along the crypt. This means that the general behavior of the IMC model well explains known experimental data. CAT, CAD, SIG, and ADH indicate the profiles of β-catenin, E-cadherin, signaling complex (β-catenin:TCF), and adhesion complex (β-catenin:E-cadherin), respectively. TRUE or FALSE indicates if the reproduced profile(s) qualitatively fits experimental data or does not fit. (J) The IMC model predicts the amount of adhesion complex is increasing along the crypt.

See also Figure S3.

gradients in the crypt facilitate the elimination of mutated cells (see Supplemental Results; Figures S4C–S4E).

Simulations of WT, APC, and β-Catenin Mutated Crypts Based on a Heterogeneous Cell Population

Our model suggests that the crypt structure enables the elimination of mutated cells that have an abnormally higher proliferation rate. To allow us to investigate this phenomenon in in vivo models, we extended this model by considering the endogenous heterogeneity of cells, which has been widely observed in various cellular contexts. In particular, we investigated the effect of heterogeneous β-catenin expression on Wnt signaling and adhesion, and the resulting repositioning of crypt cells. For this purpose, we considered a set of cells evenly sampled along

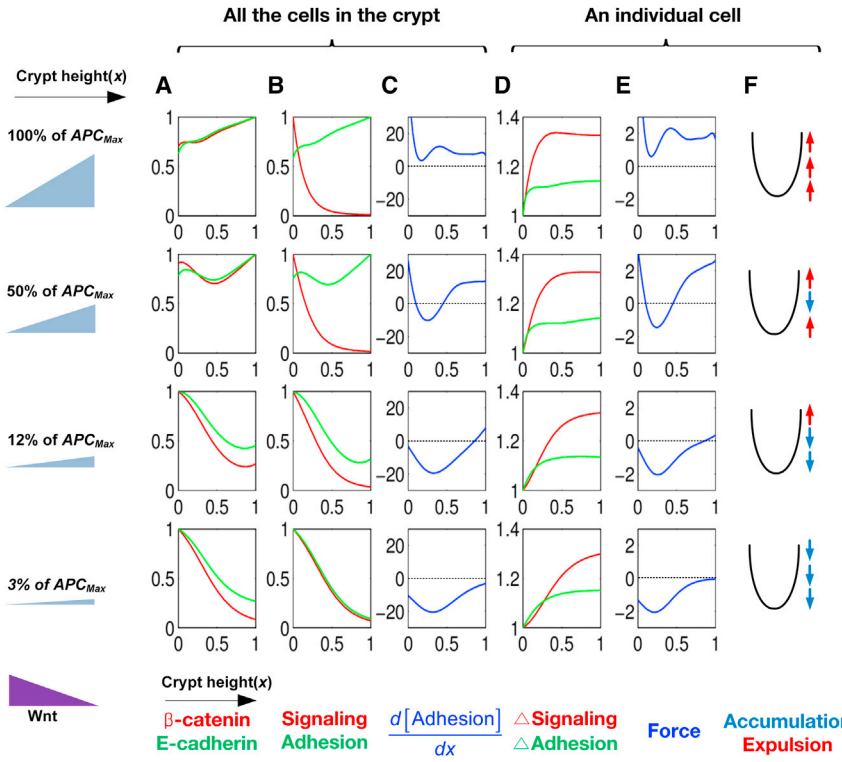

Figure 4. Simulations of the IMC Model

Simulations of the IMC model for wild-type (first row) and APC mutated (second to fourth rows) crypts. (A) and (B) are without additional Wnt stimulation and (D) is with additional Wnt stimulation. The additional Wnt stimulation is applied to mimic a cell with a higher proliferative potential.

(A and B) Simulation profiles of total β-catenin (red) and total E-cadherin (green) (A), and β-catenin:TCF signaling (red) and adhesion (green) complex (B) along the crypt. The simulation profiles are concordant with previous experiments (Wnt signaling, E-cadherin, and β-catenin) in a normal crypt (first row). In APC mutated crypts (second to fourth rows), the profiles of E-cadherin (green curve in A) and E-cadherin:β-catenin (green curve in B) became increasingly reversed compared to their profiles in the normal crypt. The total β-catenin profile (red curve in A) showed a decreasing pattern in the mutated crypt unlike the increasing pattern in the normal crypt, whereas the Wnt signaling profile (red curve in B) showed the same decreasing pattern in both normal and APC mutated crypts.

(C) The adhesion gradient was calculated numerically, and each row shows the adhesion gradient that corresponds to the adhesion curve (green) in (B).

(D) The effects of increased β-catenin on single mutated cell in a normal (first row) and APC mutated crypts (second through fourth rows) on differential adhesion (Δadhesion) and signaling (Δsignaling) before and after Wnt stimulation (50% of the maximal Wnt stimulus was added to the basal Wnt profile along the crypt). As a result, both signaling and adhesion were enhanced by the increased β-catenin in normal (first row) and APC mutated (second through fourth rows) crypts.

(E) β-catenin alterations induce differential adhesion resulting in forces that drive cell migration, which is estimated by multiplying the adhesion gradient (C) and the differential adhesion (green) in (D).

(F) Schematic summary of the changes in cell migration driven by the force field analysis shown in (E).

See also Figure S4.

the crypt axis and simulated their heterogeneous β-catenin expressions by adding random noise with the normal distribution of standard deviation ($\sigma = 0.2$) to the de novo synthesis rate of β-catenin (k_4). Such heterogeneity of β-catenin expression affects the formation of the signaling (β-catenin:TCF) and adhesion (β-catenin:E-cadherin) complexes. The change in the signaling complex affects proliferation, whereas the change of the adhesion complex results in cellular repositioning such that the difference of adhesion among neighbor cells is minimized. The repositioning eventually affects the net migration of each crypt cell. Our simulation results show such repositioning of cells (Figure 5A, fourth column) and the redistribution of cells with a high proliferative potential (Figure 5A, third column). We found that in a normal crypt, after repositioning of the cells, cells with a higher proliferative potential shift toward an upper direction, whereas cells with a lower proliferative potential shift toward a lower direction (Figure 5A, first and third columns of the first row). The average migration distance was 0.13 (cells with a higher proliferative potential) and −0.15 (cells with a lower proliferative potential), respectively (see Supplemental Results and Table S4 for details). Consequently, an intact adhesion gradient sorted crypt cells according to their proliferation rates, and cells with a higher proliferative potential incurred a penalty of reduced lifetime in crypt as shown in Figure 4. This implicates that the wild-type crypt allows cells with a lower proliferative potential to stay longer. The molecular basis of such behavior of crypt originates from the dual function of β-catenin in Wnt signaling and adhesion (Figure 1A). For instance, the increase of β-catenin increases both Wnt signaling and adhesion. Such correlated behavior is a characteristic feature of molecular interaction networks.

Next, we investigated the effects of APC and β-catenin mutation in crypt stem cells on the repositioning of crypt cells. Interestingly, the effects of APC and β-catenin mutations were not equivalent. APC mutations mainly affected the adhesion gradient (even reversed it), whereas β-catenin mutations preferentially accelerated proliferation with a lesser effect on the adhesion gradient. For a similar mutational analysis as in Figure 4, we decreased APC_{Max} by 10% (compared to its wild-type value) in the APC gradient profile to mimic a crypt having an APC mutation. We found that the fluctuations in Wnt signaling was increased by 86% (compared to wild-type), whereas that in adhesion was decreased by 69% (Figure 5A, first and second column of the second row; Supplemental Results; Table S3). As we found in Figure 4, the APC mutated crypt showed an inversion of the adhesion gradient. We also found that APC mutations increased the heterogeneity in cell proliferation rates but decreased the heterogeneity in adhesion complex formation

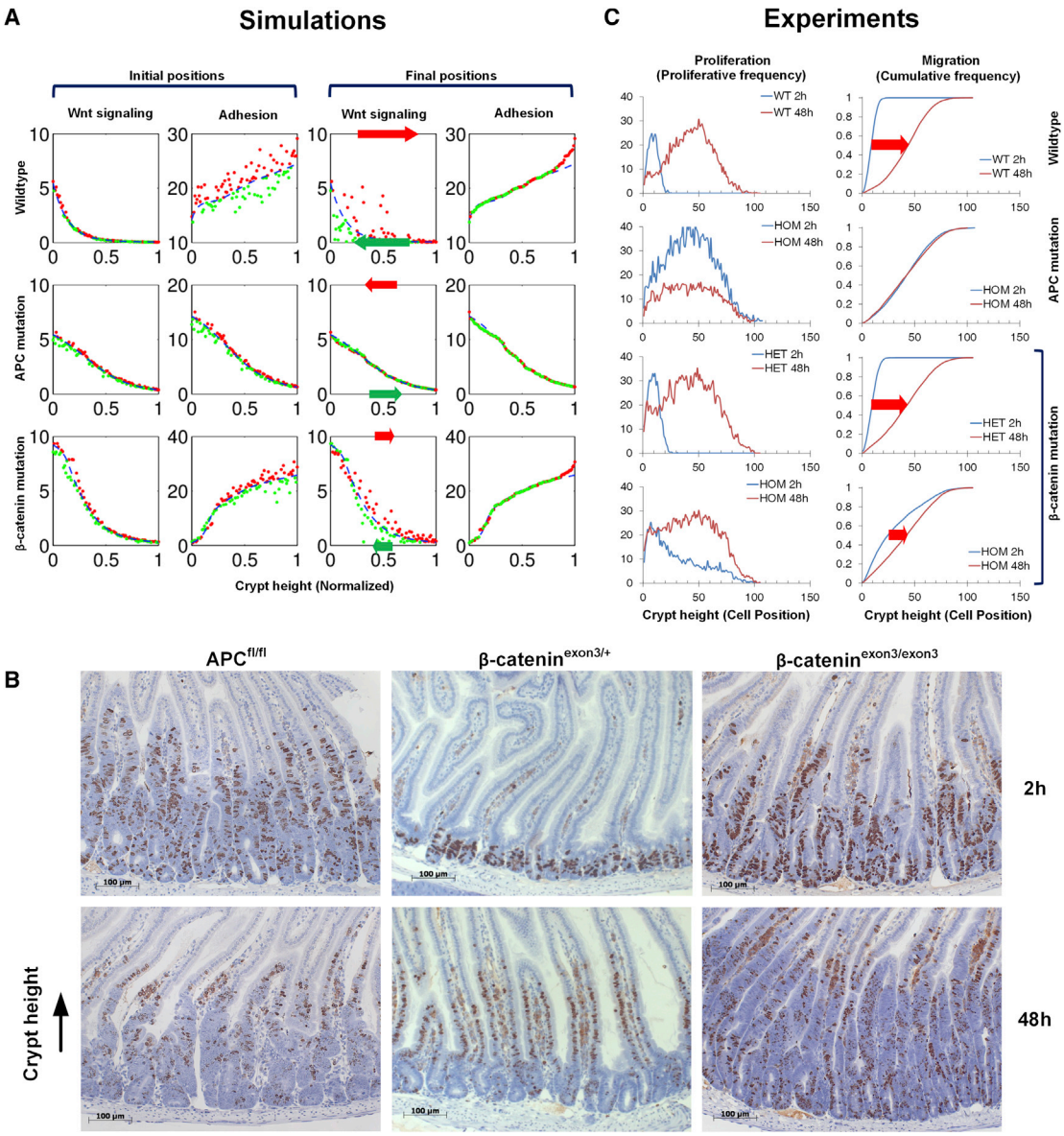

Figure 5. Experimental Testing of the Model Predictions

(A) Simulation study investigating the effect of cellular repositioning on the overall heterogeneous cell population in the wild-type crypt (first row), APC mutated crypt (second row), and β-catenin mutated crypt (third row). Here, the heterogeneity was simulated by adding random noise to the noise-free molecular profiles (blue dotted line) for 100 sampled crypt cells (first and second columns). The initial positions of the sampled crypt cells were changed to their final positions after cellular repositioning. Here, we investigated the effect of cellular repositioning on the distribution of Wnt signaling and adhesion (third and fourth columns). Red and green filled circles indicate the positive and negative deviations from the original noise-free molecular profiles. Red and green arrows indicate the migration direction and forces of red and green filled circles, respectively. To test the model predictions, we used in vivo mouse models that have homozygous APC mutation and β-catenin mutation.

(B and C) BrdU-positive cells in 2 hr following BrdU injection are confined to proliferative zones within the crypts in $APC^{fl/fl}$ (homozygous), $\beta\text{-catenin}^{exon3/+}$ (heterozygous), and $\beta\text{-catenin}^{exon3/exon3}$ (homozygous) mutated mice (B, first row). The position of BrdU-positive cells in the crypt axis 48 hr after BrdU injection, indicating migration of labeled cells toward the upper crypt (B, second row). In case of APC mutation, we used the in vivo mouse models that have homozygous mutations (C, second row). In case of β-catenin mutation, we used the in vivo mouse models that have a heterozygous mutation (C, third row) or homozygous mutations (C, fourth row). We monitored BrdU-labeled cells 2 or 48 hr after administrating BrdU as indicated. Because BrdU is incorporated for less than 2 hr postinjection, it gives an indication of the proliferative zone 2 hr postlabeling. At 48 hr, the movement and proliferation of the cells within the crypt can be monitored. We quantified the position and number of proliferative cells (C, left) and then calculated the cumulative frequency (C, right) to measure the cell migration in crypts. Therefore, when the position of the top labeled cells is scored, all events are scored, and hence the cumulative frequency equals 1.0. Arrows in (C) indicate the migration distance of BrdU-labeled cell population. Fifty half-crypts per mouse were scored for at least three different mice per genotype.

See also Tables S3, S4, S5, and S6.

caused by heterogeneous β-catenin expressions. Together, these changes resulted in the migration of cells with a higher proliferative potential toward the bottom of crypt. In our simulations, the average migration distance for cells with a higher (or lower) proliferative potential was −0.04 (0.04, respectively) (see Supplemental Results and Table S4 for details). This means that cells with a higher proliferative potential in the APC mutated crypt will greatly reduce their migration speed (toward top of the crypt) compared to cells with a lower proliferative potential, and thereby they can be accumulated in the crypt. By contrast, the cells with a lower proliferative potential increase their migration speeds (toward top of the crypt), resulting in decreased lifetime in the crypt.

Then, we investigated the effect of β-catenin mutations in stem cells on the repositioning of crypt cells. As APC mutations, β-catenin mutations are an equally important event that can cause colon cancer (Morin et al., 1997), but their incidence is comparatively very rare. It is still unclear why APC mutations are much more frequent than β-catenin mutations, although they both affect the function of the same pathway and should have similar effects when considering the textbook type wiring diagram of this pathway. Therefore, we focused our analysis on the differential effects of β-catenin versus APC mutations (see Supplemental Experimental Procedures for β-catenin mutation). As a result, we found that exon 3 mutations increase Wnt signaling along the crypt. We also found that the fluctuation of Wnt signaling becomes larger (2.67-fold), whereas the fluctuation of adhesion complex formation gets smaller (0.81-fold) compared to wild-type (Supplemental Results; Table S3). These results mean that crypt cells became more proliferative and heterogeneous, when β-catenin was mutated. However, the average migration distance of the cells with a higher proliferative potential toward the upper crypt decreased, because the fluctuation of adhesion became smaller (Figure 5A, third row, Supplemental Results; Table S3). Hence, β-catenin exon 3 mutation increases the chance to initiate cancer. In contrast to when APC is mutated, the β-catenin mutated crypt maintains the same increasing gradient of adhesion as the wild-type (Figure 5A, second column of the third row). Interestingly, the crypt with exon 3 mutation of β-catenin cannot invert the adhesion gradient as the amount of APC increases along the crypt. The inversion of the adhesion gradient facilitates cancer evolution, because it changes the migration direction of cells with a higher proliferative potential and allows them to stay longer in the crypt. From this perspective, the impact of the β-catenin mutation is much weaker than APC mutations. Cells with a higher proliferative potential shift toward upper crypt, but their average migration distance is decreased by 31% compared to the wild-type (Figure 5A, third column of third row; Supplemental Results; Table S4). Taken together, our model predicts that the migration of cells with a higher proliferative potential will be retarded in the β-catenin mutated crypt compared to the wild-type, but the retardation is less efficient than that caused by an APC mutation.

Experimental Testing of the Model Predictions

To test our model predictions in an animal model, we used genetically engineered mouse models and labeling of cells by injection of 5-bromo-2′-deoxyuridine (BrdU). BrdU is incorporated into replicating DNA (Figure 5B). Because its bioavailability is limited to <2 hr, it marks cells that were proliferating at the time of injection. However, the BrdU label remains in the DNA allowing tracking of the migration of these cells within the crypt. The first mouse model was based on the inducible deletion of APC in the intestinal epithelium (Sansom et al., 2004) (Figure 5C, second row). The second mouse model was an inducible deletion of exon 3 in β-catenin, which contains the GSK-3β phosphorylation sites and hence mimics β-catenin mutations that abolish these phosphorylation sites (Figure 5C, third and fourth rows). Both APC and β-catenin homozygous mutations strongly increased the initial distributions of proliferative frequencies as measured by counting the numbers of BrdU-positive cells 2 hr after BrdU administration (Tables S5and S6; Figure 5C, second and fourth rows). This means that both types of mutated crypts possess cells with a higher proliferative potential compared to the wild-type. We also determined the distribution of BrdU-labeled cells for the APC and the β-catenin models at 48 hr after BrdU administration and compared them to the initial distributions. In case of the APC mutated crypt, the distribution curves (Figure 5C, left of second row) and their cumulative summations (Figure 5C, right of second row) showed no difference of migration between 2 and 48 hr. These data clearly showed that the BrdU-positive cells greatly reduce their migration in the APC mutated crypt. In the case of the β-catenin mutated crypt, homozygous β-catenin mutations decreased the migration of BrdU-positive cells (Figure 5C, fourth row). However, the cumulative summations show that the BrdU-positive cells in β-catenin mutated crypt migrated faster than in the APC mutated crypt. Therefore, the experimental results show a clear agreement with the model predictions about the migration of cells with a high proliferative potential. It may appear contradictory that cells with a higher proliferative potential migrate slower in the in vivo crypt if only the mitotic pressure is considered for the migration (Heath, 1996). Our analysis provides a good explanation why it is not contradictory.

Together, our mathematical simulations combined with in vivo experimental studies show that the increase of crypt cells with a higher proliferative potential and the restructuring of the crypt environment by inverting the adhesion gradient are critical factors for cancer progression in the early stages of colon cancer development.

DISCUSSION

The critical role of APC and β-catenin mutations in the pathogenesis of CRC is well documented (Fearon, 2011; Najdi et al., 2011; Polakis, 2012; White et al., 2012). However, the molecular mechanistic consequences of these mutations are incompletely understood. Our results highlight the importance of interactions between the subcellular APC network and the adhesion and Wnt gradients in the crypt. The shuttling function of APC coordinates cell adhesion with the transcriptional activity of β-catenin, which induces genes that stimulate proliferation, such as cyclin D and c-Myc (Mosimann et al., 2009; Sansom et al., 2005). Wnt also downregulates E-cadherin expression, thereby exerting a negative feedback on the adhesion pool. This circuitry results in high Wnt responsiveness of the transcriptional function exerted by

the β-catenin:TCF complex, and in high adhesion mediated by high E-cadherin expression when APC function is also high (Figures 2D, 2E, and 2G–2J). However, at low APC levels Wnt selectively stimulated the β-catenin:TCF protein complex and inhibited E-cadherin expression. Thus, loss of APC function differentially affects the formation of the β-catenin signaling and adhesion pools in response to Wnt stimulation favoring the maintenance of the transcriptional function while reducing adhesion. Such changes support the proliferation of mutated cells with enhanced Wnt signaling and compromised APC function. These results are consistent with experimental observations suggesting that the Wnt pathway is activated in two steps during colorectal carcinogenesis, consisting of APC mutation and an additional Wnt stimulation that induces formation of the β-catenin:TCF transcription factor complex (Najdi et al., 2011). They are also consistent with the "just right" hypothesis of Wnt signaling, which is based on mutational studies and work with APC mutants expressed in transgenic mouse models. This hypothesis states that CRC can develop only if Wnt signaling is within an optimal range, and that APC mutations are selected to retain some residual functionality that can satisfy these boundary conditions (Gaspar and Fodde, 2004; Minde et al., 2011; Segditsas and Tomlinson, 2006). A plausible assumption is that such boundary conditions correlate with a major change in APC functionality. In our model, a significant change in APC functionality occurs at the border between zones 1 and 2 (Figures 2D and 2E), where Wnt maintains transcriptional activation but switches from stimulation to suppression of adhesion.

To assess potential biological consequences of such changes in APC functionality in a quantitative manner, we included the microenvironment imposed by the crypt structure into our model. We found that the normal APC expression profile along the crypt axis (i.e., decreasing from top to bottom) is critical to maintain a proper adhesion profile along the crypt that allows cells to migrate up to the top of the crypt and be shed into the lumen. Individual cells adjust their positions to minimize the total sum of the adhesion differences between themselves and their neighbors (Steinberg, 2007). Our simulations showed that this differential adhesion forces in a normal crypt push mutated cells with enhanced Wnt signaling upward, resulting in the elimination of mutant cells. The overall directionality of the adhesion gradient pushing cells upward is preserved as long as APC function is $\geq$50%, which corresponds to a heterozygous situation. Thus, the removal of mutated cells could be maintained for prolonged periods of time, which is consistent with the long latency period between APC mutations and CRC development (Fearon, 2011). However, if APC function in the crypt drops to $\leq$12%, the adhesion gradient reverses allowing mutated cells to stay in the crypt and continue proliferating. Quantitatively, these data fit well with the approximately 10-fold reduction in APC function that marks the border between zones 1 and 2 in Figures 2D and 2E.

Therefore, we conclude that the spatial distribution of APC and formation of an adhesion gradient in the crypt is critical for the tumor suppressor function of APC, and that at the level of an individual cell the coordination between the signaling and adhesion function is quite resilient to the heterozygous loss of APC function.

In summary, our system's biological approach revealed how intracellular signaling, the anatomical structure of the crypt, and adhesion gradients combine to provide a tissue homeostasis strategy that safeguards against tumorigenesis by promoting the removal of mutated and hyperproliferative cells. Although our model captures salient aspects of this homeostasis, it—like any model—is an abstraction that allows us to reduce complex phenomena to reveal underlying principles. The current model is a solid foundation for expansion by considering further aspects such as cell differentiation, apoptosis, and the relationship between mutations in stem cells or transit amplifying cells.

EXPERIMENTAL PROCEDURES

Mathematical Modeling

We considered six key molecular species, APC, Axin, β-catenin, TCF, E-cadherin, and Slug, and the extracellular Wnt stimulus as input and employed ordinary differential equations to develop a mathematical model of the molecular interactions (see Supplemental Experimental Procedures for details) (Cho et al., 2003; Cho and Wolkenhauer, 2003). The system equations were numerically integrated using SUNDIALS solvers (https://computation.llnl.gov/casc/sundials/main.html).

Experimental Testing Using In Vivo Models

All experiments were performed under the UK Home Office guidelines. Outbred mice segregating for the C57BL6J and S129 genomes from 6 to 12 weeks of age were used. The following alleles were used: $Apc^{580Sflox}$ (Sansom et al., 2004), $Catnb^{lox(ex3)}$ (Harada et al., 1999), AhCre (Ireland et al., 2004), AhCreER (Kemp et al., 2004). To induce recombination, mice were given 3 × 80 mg/kg β-naphthoflavone in one single day (AhCre) or 2 × 80 mg/kg/day β-naphthoflavone/tamoxifen for 2 days. Mice were examined 4 days ($AhCre^{+}$ $Apc^{fl/fl}$ 2 hr BrdU), 5 days ($AhCre^{+}$ $Apc^{fl/fl}$ 48 hr BrdU) or 5 days ($AhCreER^{+}$ $Catnb^{lox(ex3)/+}$ and $Catnb^{lox(ex3)/lox(ex3)}$, 2 hr, and 48 hr BrdU) after the first injection. For BrdU labeling, mice were injected either 2 or 48 hr prior to sacrifice with 0.25 ml BrdU (GE Healthcare). The small intestine was harvested and fixed in methacarn (methanol, chloroform, and acetic acid; 4:2:1). Staining for BrdU was performed using an anti-BrdU conjugate (BD Biosciences, 1:200). Cells were counted along the crypt-villus axis from the bottom of the crypt until the last BrdU-positive cell and scored with 0 or 1 for BrdU positivity. At least 50 half-crypts per mouse were scored and three to four mice per genotype. The cumulative frequency was calculated as described previously (Sansom et al., 2004). The detailed scoring data can be found in Tables S5 and S6.

SUPPLEMENTAL INFORMATION

Supplemental Information includes Supplemental Experimental Procedures, Supplemental Results, four figures, and six tables and can be found with this article online at http://dx.doi.org/10.1016/j.celrep.2014.02.043.

ACKNOWLEDGMENTS

The authors thank Dongkwan Shin and Tae-Hwan Kim for their helpful discussion. This work was supported by the National Research Foundation of Korea (NRF) grants funded by the Korean Government, the Ministry of Science, ICT & Future Planning (2010-0017662). W.K. acknowledges the support by the Science Foundation Ireland under grant no. 06/CE/B1129. O.J.S. acknowledges the support received from a CrUK core grant and an ERC starter grant "Coloncan." D.J.H. is supported by the EU FP7 grant no. 278568 "PRIMES."

Received: July 30, 2013
Revised: February 3, 2014
Accepted: February 26, 2014
Published: March 27, 2014

REFERENCES

Azcárate-Peril, M.A., Sikes, M., and Bruno-Bárcena, J.M. (2011). The intestinal microbiota, gastrointestinal environment and colorectal cancer: A putative role for probiotics in prevention of colorectal cancer? Am. J. Physiol. *301*, G401–G424.

Brabletz, T., Jung, A., Hermann, K., Günther, K., Hohenberger, W., and Kirchner, T. (1998). Nuclear overexpression of the oncoprotein beta-catenin in colorectal cancer is localized predominantly at the invasion front. Pathol. Res. Pract. *194*, 701–704.

Cho, K.H., and Wolkenhauer, O. (2003). Analysis and modelling of signal transduction pathways in systems biology. Biochem. Soc. Trans. *31*, 1503–1509.

Cho, K.-H., Shin, S.-Y., Lee, H.-W., and Wolkenhauer, O. (2003). Investigations into the analysis and modeling of the TNF alpha-mediated NF-kappa B-signaling pathway. Genome Res. *13*, 2413–2422.

Cho, K.-H., Baek, S., and Sung, M.-H. (2006). Wnt pathway mutations selected by optimal beta-catenin signaling for tumorigenesis. FEBS Lett. *580*, 3665–3670.

Davies, P.S., Dismuke, A.D., Powell, A.E., Carroll, K.H., and Wong, M.H. (2008). Wnt-reporter expression pattern in the mouse intestine during homeostasis. BMC Gastroenterol. *8*, 57.

Diggs, D.L., Huderson, A.C., Harris, K.L., Myers, J.N., Banks, L.D., Rekhadevi, P.V., Niaz, M.S., and Ramesh, A. (2011). Polycyclic aromatic hydrocarbons and digestive tract cancers: a perspective. J Environ Sci Health C Environ Carcinog Ecotoxicol Rev *29*, 324–357.

Fearon, E.R. (2011). Molecular genetics of colorectal cancer. Annu. Rev. Pathol. *6*, 479–507.

Ferlay, J., Shin, H.R., Bray, F., Forman, D., Mathers, C., and Parkin, D.M. (2010). GLOBOCAN 2008 v1.2: Cancer Incidence and Mortality Worldwide: IARC CancerBase No. 10. Lyon (France): IARC Press. http://globocan.iarc.fr.

Fodde, R., Smits, R., and Clevers, H. (2001). APC, signal transduction and genetic instability in colorectal cancer. Nat. Rev. Cancer *1*, 55–67.

Gaspar, C., and Fodde, R. (2004). APC dosage effects in tumorigenesis and stem cell differentiation. Int. J. Dev. Biol. *48*, 377–386.

Gatenby, R.A., Gillies, R.J., and Brown, J.S. (2010). Evolutionary dynamics of cancer prevention. Nat. Rev. Cancer *10*, 526–527.

Harada, N., Tamai, Y., Ishikawa, T., Sauer, B., Takaku, K., Oshima, M., and Taketo, M.M. (1999). Intestinal polyposis in mice with a dominant stable mutation of the beta-catenin gene. EMBO J. *18*, 5931–5942.

Heath, J.P. (1996). Epithelial cell migration in the intestine. Cell Biol. Int. *20*, 139–146.

Herzig, M., Savarese, F., Novatchkova, M., Semb, H., and Christofori, G. (2007). Tumor progression induced by the loss of E-cadherin independent of β-catenin/Tcf-mediated Wnt signaling. Oncogene *26*, 2290–2298.

Humphries, A., and Wright, N.A. (2008). Colonic crypt organization and tumorigenesis. Nat. Rev. Cancer *8*, 415–424.

Ireland, H., Kemp, R., Houghton, C., Howard, L., Clarke, A.R., Sansom, O.J., and Winton, D.J. (2004). Inducible Cre-mediated control of gene expression in the murine gastrointestinal tract: effect of loss of β-catenin. Gastroenterology *126*, 1236–1246.

Kemp, R., Ireland, H., Clayton, E., Houghton, C., Howard, L., and Winton, D.J. (2004). Elimination of background recombination: somatic induction of Cre by combined transcriptional regulation and hormone binding affinity. Nucleic Acids Res. *32*, e92.

Minde, D.P., Anvarian, Z., Rüdiger, S.G., and Maurice, M.M. (2011). Messing up disorder: how do missense mutations in the tumor suppressor protein APC lead to cancer? Mol. Cancer *10*, 101–101.

Morin, P.J., Sparks, A.B., Korinek, V., Barker, N., Clevers, H., Vogelstein, B., and Kinzler, K.W. (1997). Activation of β-catenin-Tcf signaling in colon cancer by mutations in β-catenin or APC. Science *275*, 1787–1790.

Mosimann, C., Hausmann, G., and Basler, K. (2009). Beta-catenin hits chromatin: regulation of Wnt target gene activation. Nat. Rev. Mol. Cell Biol. *10*, 276–286.

Murray, P.J., Kang, J.-W., Mirams, G.R., Shin, S.-Y., Byrne, H.M., Maini, P.K., and Cho, K.-H. (2010). Modelling spatially regulated beta-catenin dynamics and invasion in intestinal crypts. Biophys. J. *99*, 716–725.

Muzny, D.M., Bainbridge, M.N., Chang, K., Dinh, H.H., Drummond, J.A., Fowler, G., Kovar, C.L., Lewis, L.R., Morgan, M.B., Newsham, I.F., et al.; Cancer Genome Atlas Network (2012). Comprehensive molecular characterization of human colon and rectal cancer. Nature *487*, 330–337.

Najdi, R., Holcombe, R.F., and Waterman, M.L. (2011). Wnt signaling and colon carcinogenesis: beyond APC. J. Carcinog. *10*, 5.

Nowak, M.A., Michor, F., and Iwasa, Y. (2003). The linear process of somatic evolution. Proc. Natl. Acad. Sci. USA *100*, 14966–14969.

Okamoto, R., and Watanabe, M. (2004). Molecular and clinical basis for the regeneration of human gastrointestinal epithelia. J. Gastroenterol. *39*, 1–6.

Pearson, J.R., Gill, C.I., and Rowland, I.R. (2009). Diet, fecal water, and colon cancer—development of a biomarker. Nutr. Rev. *67*, 509–526.

Phelps, R.A., Broadbent, T.J., Stafforini, D.M., and Jones, D.A. (2009). New perspectives on APC control of cell fate and proliferation in colorectal cancer. Cell Cycle *8*, 2549–2556.

Polakis, P. (2012). Drugging Wnt signalling in cancer. EMBO J. *31*, 2737–2746.

Powell, S.M., Zilz, N., Beazer-Barclay, Y., Bryan, T.M., Hamilton, S.R., Thibodeau, S.N., Vogelstein, B., and Kinzler, K.W. (1992). APC mutations occur early during colorectal tumorigenesis. Nature *359*, 235–237.

Sansom, O.J., Reed, K.R., Hayes, A.J., Ireland, H., Brinkmann, H., Newton, I.P., Batlle, E., Simon-Assmann, P., Clevers, H., Nathke, I.S., et al. (2004). Loss of Apc in vivo immediately perturbs Wnt signaling, differentiation, and migration. Genes Dev. *18*, 1385–1390.

Sansom, O.J., Reed, K.R., van de Wetering, M., Muncan, V., Winton, D.J., Clevers, H., and Clarke, A.R. (2005). Cyclin D1 is not an immediate target of beta-catenin following Apc loss in the intestine. J. Biol. Chem. *280*, 28463–28467.

Segditsas, S., and Tomlinson, I. (2006). Colorectal cancer and genetic alterations in the Wnt pathway. Oncogene *25*, 7531–7537.

Steinberg, M.S. (2007). Differential adhesion in morphogenesis: a modern view. Curr. Opin. Genet. Dev. *17*, 281–286.

van de Wetering, M., Sancho, E., Verweij, C., de Lau, W., Oving, I., Hurlstone, A., van der Horn, K., Batlle, E., Coudreuse, D., Haramis, A.P., et al. (2002). The beta-catenin/TCF-4 complex imposes a crypt progenitor phenotype on colorectal cancer cells. Cell *111*, 241–250.

White, B.D., Chien, A.J., and Dawson, D.W. (2012). Dysregulation of Wnt/β-catenin signaling in gastrointestinal cancers. Gastroenterology *142*, 219–232.